Compatibility of braiding and fusion on wire networks

A. Conlon [*] and J. K. Slingerland [†]
Department of Theoretical Physics, Maynooth University, Dublin W23 F2H6, Ireland
and School of Theoretical Physics, Dublin Institute for Advanced Studies, 10 Burlington Road, Dublin 4, D04 C932, Ireland

(Received 4 March 2022; revised 5 August 2022; accepted 23 June 2023; published 27 July 2023)

Exchanging particles on graphs, or more concretely on networks of quantum wires, has been proposed as a means to perform fault-tolerant quantum computation. This was inspired by braiding of anyons in planar systems. However, exchanges on a graph are not governed by the usual braid group but instead by a graph braid group. By imposing compatibility of graph braiding with fusion of topological charges, we obtain generalized hexagon equations. We find the usual planar anyon solutions but also more general braid actions. We illustrate this with Abelian, Fibonacci, and Ising fusion rules.

DOI: 10.1103/PhysRevB.108.035150

I. INTRODUCTION

Two decades ago, it was realized that an inherently fault-tolerant quantum computation scheme could be implemented using the exchange statistics of anyons, quasiparticles in planar systems. This gave birth to the field of *topological quantum computation* (TQC) [1–3]. Physical systems that can host anyons include fractional quantum Hall (FQH) states [4]. In fact, the Aharonov-Bohm signature of Abelian anyon exchange statistics in FQH states was recently directly observed [5,6]. Much of the effort in TQC has recently focused on one-dimensional systems since it was proposed [7] that the braiding of anyonlike excitations could be performed at junctions in networks of semiconductor wires. The possibility of transporting Majorana modes around networks has been extensively investigated [8–18]. There have also been similar proposals for parafermionic excitations [19,20]. Exchanging particles on networks, or graphs, rather than in the plane, merits closer investigation. The exchange statistics of N identical particles are governed by the representations of the fundamental group of the configuration space of the system. This is the space of unordered collections of N distinct particle positions in the relevant geometry [21–23]. For particles on the plane this fundamental group is the braid group B_N, while in three-dimensional space we obtain the permutation group S_N, leading to bosons and fermions. For particles moving on graphs, we can obtain a variety of exchange groups, dubbed graph braid groups. These have recently been analyzed in some detail in [24–26] and appear to be the natural tool to study the exchange statistics of particles on wire networks, without reference to a two-dimensional medium. Given that anyons can be braided while restricting their motion to planar graphs, the corresponding representations of B_N must appear also as a representation of a planar graph braid group. For sufficiently connected planar graphs, graph braids satisfy the same relations as braids on the plane or surface.

However, for less connected graphs, such as a trijunction, graph braiding affords more freedom and it has been conjectured [25,27] that there may be braid statistics on a graph which do not exist in the plane. In fact, for simple junctions, graph braid groups are free groups, allowing for arbitrary braid actions on the Hilbert space. This strongly suggests that more physical input is needed to pick specific graph braid representations. An important piece of information we can add is the fusion of the particles' topological charges. For anyons, this leads to the framework of anyon models, or more precisely unitary braided tensor categories. The braiding is constrained through the hexagon equations, which enforce compatibility of braiding and fusion. We now develop the basics of an analogous framework for particles on graphs.

II. QUANTUM EXCHANGE STATISTICS AND GRAPH BRAID GROUPS

The N-strand graph braid group $B_N(\Gamma)$ of a graph Γ is defined [24–26] by $B_N(\Gamma) = \pi_1(C_N(\Gamma))$. Here $C_N(\Gamma)$ is the space of configurations of N identical particles in distinct positions on Γ. For convenience we take the base point so that all particles are located on a single edge of the graph. A graph braid is then represented by the space-time history where the particles start at their positions on this initial edge, are then transported to other edges, and finally returned to the initial edge, possibly with the order of some of the particles changed. An example of a two-particle exchange at a trijunction can be seen in Fig. 1. Clearly, each junction in the graph offers an opportunity to exchange particles in this way. An intuitive presentation of $B_N(\Gamma)$ based on two-particle exchanges is given in [26]. This presentation has generators denoted by $\sigma_j^{(a_1,a_2,\ldots,a_j,a_{j+1})}$, where a_i denotes the edge that the ith particle away from the junction point is moved to during the graph braid. For general graphs one makes this unambiguous by first choosing a unique path out to each edge. This is provided by the spanning tree of the graph. The subscript j denotes that after the action of σ_j the particles return to the initial edge in the same ordering except that particle $j+1$ returns before particle j, so that these particles end up on the initial

[*] aaron@stp.dias.ie
[†] joost@thphys.nuim.ie

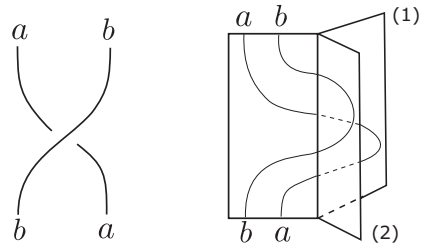

FIG. 1. Diagrams for a simple two-particle exchange on the plane τ_1 (left) and on a trijunction $\sigma_1^{(1,2)}$ (right).

edge in reverse order. Note that in exchanging particle j with particle $j+1$, it is necessary to move all particles ahead of particle j in order to get particle j to a vertex, where it can then be exchanged. The inverse of a σ_j generator is given by switching a_j and a_{j+1}. We can contrast these generators with the well-known presentation of the planar braid group B_N generated by τ_i, which exchanges two neighboring strands labeled i and $i+1$, subject to the following relations:

$$\tau_i\tau_j = \tau_j\tau_i \quad |j-i| \geqslant 2 \quad \text{and} \quad \tau_{i+1}\tau_i\tau_{i+1} = \tau_i\tau_{i+1}\tau_i. \quad (1)$$

We may call these relations the local commutativity (left) and Yang-Baxter relations (right). All the $\sigma_j^{(a_1,a_2,\ldots,a_j,a_{j+1})}$ operators would correspond either to τ_j or to τ_j^{-1} if the particles were free to move in the plane, but when motion is restricted to the graph, it is necessary to keep track of the edges where the rest of the particles that are moved out of the way go to during the motion and as a result graph braid groups have multiple counterpart generators for τ_j with $j > 1$.

In general, graph braid groups have fewer relations than the planar braid group in the following sense [25,26]. For some, but not all, pairs of σ_i, σ_j generators (depending on the upper indices) there are relations similar to local commutativity (these are called pseudocommutative relations) and similarly for some σ_j generators there are relations analogous to the braid relation (called pseudobraid relations). The overall structure of graph braid groups is often quite simple. For example, if the graph has one vertex and d edges, the graph braid group is isomorphic to a free group. Some of the σ_j generators can be eliminated, depending on d, but a number remain and those have no further relations. This means these generators can be represented by any unitary operators on the Hilbert space and more physical information will be needed to actually determine the effect of particle exchanges. We shall focus on $N = 3$ particles on a trijunction. This is one of the most familiar setups for TQC, [7,16,18,19]. The graph braid group is generated by

$$B_3(\Gamma_3) = \langle \sigma_1^{(1,2)}, \quad \sigma_2^{(2,1,2)}, \quad \sigma_2^{(1,1,2)} \rangle. \quad (2)$$

In this case there are no pseudocommutative relations and it can be verified graphically that there are no pseudobraid relations either because the required path deformation would require two particles to occupy the vertex simultaneously, which is forbidden. Hence, $B_3(\Gamma_3)$ is a free group on three generators and we need more physical input to constrain the unitary operators which implement exchanges. To this end we introduce topological charges and fusion into the picture.

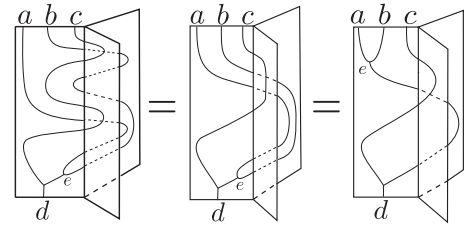

FIG. 2. Here we show an example of sliding a fusion vertex $e = a \times b$ through a graph braid.

III. GRAPH ANYON MODELS

We now construct the elements of graph anyon models, analogous to the planar braiding of anyons (see, e.g., [2,28]). A more complete presentation will be given in [29]. Particles in a graph anyon model carry one of a finite set of topological charges $a, b, c, \ldots$, there is fusion of charges

$$a \times b = \sum_c N_c^{ab} c. \quad (3)$$

The coefficient $N_c^{ab} \in \mathbb{Z}_{\geqslant 0}$ is the dimension of the fusion space V_c^{ab} of ground states on a single edge, with two particles of charges a and b and with overall charge c. Here, we will consider only multiplicity free models, so $N_c^{ab} \in \{0, 1\}$. There is a unique vacuum charge 1, such that $a \times 1 = 1 \times a = a$ for all a. Also, each charge a has a unique conjugate $a \times \bar{a} = 1 + \cdots$. We choose an orthonormal basis for each nontrivial fusion space V_c^{ab}. This choice introduces a gauge freedom u_c^{ab}, a unitary matrix of dimension N_c^{ab} which changes the basis and leaves the physics unchanged. In the multiplicity free case, $u_c^{ab} \in \mathrm{U}(1)$. We can form multiparticle states from tensor products of fusion spaces. This leads to two alternative bases for the three-particle space of charges a, b, c with total topological charge d, related by a change of basis whose matrix elements $[F_d^{abc}]_{e,f}$ are called the F symbols:

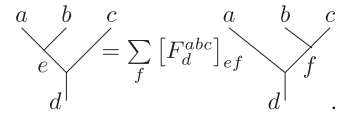

The F symbols are required to satisfy the *pentagon equation*, which ensures that the order of fusion can be consistently rearranged locally for systems with any number of particles [2,28]. The description of braiding in planar anyon models is implemented by a unitary operation R. Its effect on V_c^{ab} is given by the R *symbols* R_c^{ab} which are U(1) matrices. The compatibility of fusion and braiding is often phrased by saying that *fusion commutes with braiding*. In space-time diagrams it means that we can slide a particle world line under or over a fusion or splitting vertex. To make this consistent, the R symbols must satisfy the *hexagon equations*. For braiding on a graph, the usual hexagon equations are not valid, in fact, fusion and braiding do not always commute. However, there are still particular processes where a continuous deformation of the particles' history leads to an exchange of a fusion with a braiding in time (see Fig. 2 for an example). We now define appropriate symbols satisfying graph hexagon equations which express this remaining consistency of fusion and

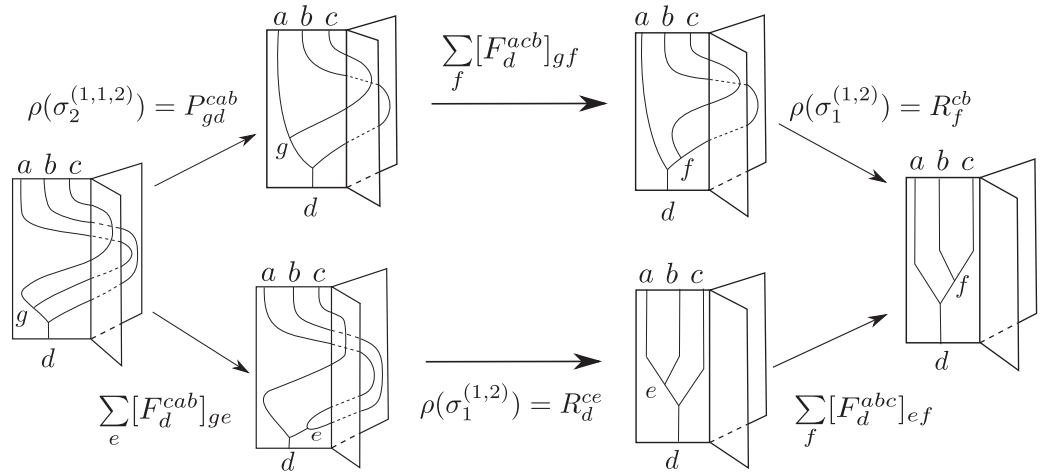

FIG. 3. Here we show a hexagonal commutative diagram enforcing compatibility of fusion and graph braiding. In the bottom left state we have used the premise that fusion commutes with graph braiding, which we display in Fig. 2.

braiding on a trijunction:

$$\rho\left(\sigma_1^{(1,2)}\right) := R, \quad \rho\left(\sigma_2^{(2,1,2)}\right) := Q, \quad \rho\left(\sigma_2^{(1,1,2)}\right) := P. \quad (4)$$

The action of R on V_c^{ab} is given by R symbols

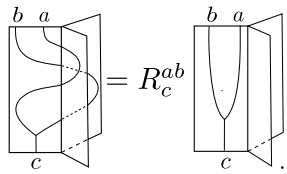

Note these R symbols are not necessarily solutions of the planar hexagon equations. Similarly, the graphical representations of P and Q, which exchange the second and third particles away from the vertex, are

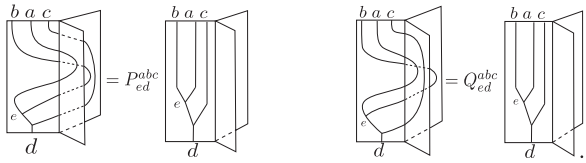

Note that these braiding processes necessarily involve all three particles labeled a, b, c and so we have introduced additional labels characterizing the full three-particle state to label matrix elements of the graph braid matrices. If we made P and Q only depend on a, b and their fusion outcome, we would have $P = Q$, despite the fact they represent different generators in the graph braid group. As in the planar case, the P, Q, R symbols are U(1) matrices acting on the states of V_c^{ab}. Gauge transformations, as discussed in [2], have a similar effect on P, Q, and R, and we have

$$R_c^{ab'} = \frac{u_c^{ba}}{u_c^{ab}} R_c^{ab}, \quad W_{ed}^{abc'} = \frac{u_e^{ba}}{u_e^{ab}} W_{ed}^{abc}, \quad W \in \{P, Q\}. \quad (5)$$

We now consider compatibility of graph braiding and fusion. If a particle braids over two other particles with a given total charge (fusion channel), the process must involve two individual exchanges (see Fig. 2). Here, the two exchanges are such that we can *slide* a fusion vertex through a graph braid. This implies in particular that the two particles with the joint charge e must go to the same edge during the braid process. Otherwise, the move pushing the splitting vertex upward would be blocked at the graph's vertex and it would not pass under the world line of charge c.

Adapting the notation from the σ presentation, we can write an equation for the diagram identity in Fig. 2 as follows:

$$\sigma_2^{(1_b,1_a,2_c)} \circ \sigma_1^{(1_b,2_c)} = \sigma_1^{(1_{b\times a},2_c)} = \sigma_1^{(1_e,2_c)}. \quad (6)$$

We can now construct our consistency equations for graph braiding and fusion: the graph hexagon equations. We note that we can connect the two sides of the identity in Fig. 2 by a series of F moves and exchanges and we then require this combination of moves to be the identity. This leads to the hexagonal commutative diagram in Fig. 3. We can similarly obtain another such equation in a situation where the joined particles move to the other plane. This leads to the equations

$$P_{gd}^{cab} \left[F_d^{acb}\right]_{gf} R_f^{cb} = \sum_e \left[F_d^{cab}\right]_{ge} R_d^{ce} \left[F_d^{abc}\right]_{ef},$$
$$\left(Q_{gd}^{acb}\right)^* \left[F_d^{acb}\right]_{gf} \left(R_f^{bc}\right)^* = \sum_e \left[F_d^{cab}\right]_{ge} \left(R_d^{ec}\right)^* \left[F_d^{abc}\right]_{ef}. \quad (7)$$

Of course, similar equations can also be derived starting from the inverse braids. These are equivalent to the ones given and involve P^{-1} and Q. We can also check that the equations are consistent with simple physical requirements such as $P_{ac}^{1ab} = P_{ac}^{a1b} = 1$ and $P_{cc}^{ab1} = R_c^{ab}$, and similarly for Q.

IV. SOLUTIONS OF THE GRAPH HEXAGON EQUATIONS

First of all, we note that, when $P_{ed}^{abc} = Q_{ed}^{abc} = R_e^{ab}$, for all a, b, c, d, e, the graph hexagons reduce to the usual hexagon equations for planar systems, and the corresponding graph braid group representations are necessarily representations of B_N. Hence, any planar anyon model immediately provides solutions to these equations, although often further solutions exist. We now consider some simple fusion models to illustrate what else is possible. Since the graph braid matrices and F matrices are invertible, we can immediately use the hexagon equations (7) to express the P and Q symbols in terms of the R symbols. This means we only need to supply the F symbols

and find the R_c^{ab} to fix all symbols. Notice that we usually get multiple expressions for the same P or Q symbol, as the index f varies. This will restrict the possible values for the R_c^{ab}. However, in Abelian fusion models, given F, the R_c^{ab} are not restricted and can be freely chosen. In such models, the charges $a, b, \ldots$ are elements of a finite Abelian group G and the fusion corresponds to group multiplication, giving a unique outcome for each fusion. In this case the label f in Eq. (7) is fixed as the unique fusion of b and c. Hence a choice of $R_{a\times b}^{ab}$ just fixes the P and Q symbols. There are no requirements on R, apart from $R_c^{ab} \in \mathrm{U}(1)$ and $R_a^{a1} = R_a^{1a} = 1$. This already gives us many examples which do not satisfy the planar hexagon equations. For example, when $G = \mathbb{Z}_M$, the F symbols satisfying the pentagon equations are given by 3-cocycle ω in the group cohomology of G [28]. The solutions R_c^{ab} to the planar hexagons for $\mathbb{Z}_M^{\omega}$ with trivial ω are required to form a nondegenerate symmetric bicharacter $\chi(a, b)$, but no such requirement is needed on a graph. Perhaps more interestingly, there is often no nontrivial solution to the planar hexagon. This occurs, e.g., for bosonic topological order when M is odd and $\omega(a, b, c)$ is cohomologically nontrivial [30]. Nevertheless, there is a solution for any choice of the $R_{a\times b}^{a,b}$ on the trijunction and so we can graph braid particles that do not permit planar braiding. Overall, for any group G we obtain a $(|G| - 1)^2$ parameter family of solutions for any fixed choice of F symbols. Some of these will be related through the gauge freedom (5). However, since the symbols $R_{a\times a}^{aa}$ and the products $R_{a\times b}^{ab}R_{b\times a}^{ba}$ are independent and gauge invariant for all $a, b \neq 1$, we always have at least $|G|(|G| - 1)/2$ physical parameters. For theories with non-Abelian braiding we must equate the expressions for P and Q which come from different choices of f in Eq. (7). This then yields equations purely for R_c^{ab}. For example, for the Fibonacci model, which has a single nontrivial charge τ with $\tau \times \tau = 1 + \tau$, we recover the known planar values for the R symbols as the only solutions, and $P_{ed}^{abc} = Q_{ed}^{abc} = R_e^{ab}$. Another important example is the Ising theory: this model is directly relevant for topological memories based on quantum wires that host Majorana modes [7,12], although it is not universal for quantum computation by braiding alone [31,32]. The Ising theory is an example of a larger family known as the Tambara-Yamagami models [33]. We have charges g_i forming a finite Abelian group G and a single additional charge σ such that $\sigma \times \sigma = \sum_i g_i$ and $g_i \times \sigma = \sigma$. The case $G = \mathbb{Z}_2$ is the Ising model with $(1, \sigma, \psi) \equiv (g_0, \sigma, g_1)$ being the more usual notation. All these fusion rules have known F symbols, but in the plane they allow no solutions to the hexagon equations unless $G = (\mathbb{Z}_2)^n$ for some n [34]. We find there is similarly no solution to the graph hexagon equations unless $G = \mathbb{Z}_2^n$ [29]. However, when $G = \mathbb{Z}_2^n$ graph braid solutions without a counterpart in the plane exist. We state some results for the Ising model. There are two possible solutions of the pentagon equations, but it turns out that these lead to the same set of R symbols for the graph hexagon equations, namely,

$$R_{\psi}^{\sigma\sigma} = \mp i R_1^{\sigma\sigma}, \quad R_{\sigma}^{\sigma\psi} = R_{\sigma}^{\psi\sigma} = \pm i, \quad R_1^{\psi\psi}, R_1^{\sigma\sigma} \in \mathrm{U}(1). \tag{8}$$

These solutions are inequivalent under gauge transformations which fix the F symbols. The free parameters $R_1^{\psi\psi}$ and $R_1^{\sigma\sigma}$ are gauge invariant. The planar Ising solutions appear for $R_1^{\psi\psi} = -1$ and $R_1^{\sigma\sigma} = e^{\pm i(2k+1)\pi/8}$, where $k \in \{0, 1, 2, 3\}$.[1] The P and Q symbols are now easily obtained, and given in Appendix B. They depend on the chosen pentagon solution.

V. DISCUSSION AND OUTLOOK

We have presented only the basic features of braiding and fusion on graphs here, stressing the differences with planar systems. In [29], we consider general networks with more and higher valence vertices and loops, and with more particles braiding, as well as further implications for TQC. As a taster, we work out the case of three particles on a 4-valent junction in Appendix A, focusing on the effect of the pseudobraid relation which first appears there. Many features presented here persist generally, for example, using compatibility of braiding and fusion we can always express generators σ_j for exchanges of particles further from the vertex in terms of exchanges $\sigma_{j'<j}$ of those closer to the vertex (though details depend on the valence). An interesting question is to find a generating set for all compatibility constraints for braiding and fusion for any number of particles on any graph. This may be most elegantly addressed in a categorical setting where it would lead to an analog of the MacLane coherence theorem [35]. Another natural question is under what circumstances the coherence is strong enough to yield Ocneanu rigidity [2,36], meaning that the set of solutions modulo gauge is finite. This clearly does not hold for the trijunction, but this property returns for networks with loops. Finally, in Appendix C, to provide an additional insight into graph braiding of topological excitations, in Appendix C, we introduce a local model of quasiparticles exchanging at a trijunction. We show that it recovers non-planar solutions of the graph braiding hexagon equations.

ACKNOWLEDGMENTS

The authors would like to extend special gratitude to Dr. T. Maciążek for introducing the authors to this topic. J.K.S. acknowledges financial support from Science Foundation Ireland through Principal Investigator Awards No. 12/IA/1697 and No. 16/IA/4524. A.C. was supported through IRC Government of Ireland Postgraduate Scholarship GOIPG/2016/722. The authors acknowledge financial support from the Heilbronn Institute for Mathematical Research, who facilitated a workshop on this topic, titled "Representations of Graph Braid Groups in Topological Quantum Computing". A.C. would like to thank Dr. I. Jubb for helpful discussions.

APPENDIX A: TETRAJUNCTION

The tetrajunction Γ_4 is one of the simplest graphs for which the graph braid group contains a pseudobraid relation. Additionally, we can observe that $B_3(\Gamma_4)$ contains three subtrijunctions, coming from assigning the particles to an initial

[1] Note that on the plane, the cases $k = 0$ and $k = 3$ occur for one set of F symbols while the remaining cases occur for the other set. Here, all options occur for either choice of F symbols.

edge and then choosing one of the three choices of pairs of the remaining three edges to exchange them. The graph braid group $B_3(\Gamma_4)$ is a free group of rank 11, but there are 12 elements in the σ presentation. One of these can be eliminated by means of the pseudobraid relation [26]. The matrices representing the generators of $B_3(\Gamma_4)$ can be written as

$$\begin{aligned}
\rho\left(\sigma_1^{(1,2)}\right) &:= X, \quad \rho\left(\sigma_2^{(a_1,1,2)}\right) = X_{a_1}, \\
\rho\left(\sigma_1^{(2,3)}\right) &:= Y, \quad \rho\left(\sigma_2^{(a_1,2,3)}\right) = Y_{a_1}, \\
\rho\left(\sigma_1^{(1,3)}\right) &:= Z, \quad \rho\left(\sigma_2^{(a_1,1,3)}\right) = Z_{a_1}.
\end{aligned} \tag{A1}$$

Here, $a_1 \in \{1, 2, 3\}$ labels the edge that the particle closest to the junction point goes to during the graph braid. This notation highlights the trijunction subgroups. Referring to the notation used for the trijunction in Eq. (4) in the main text, we see that the R matrices (given by exchanging the two particles closest to the junction point) for each subtrijunction occur in the first column above and are now labeled X, Y, and Z for the three trijunctions. The P and Q graph braid matrices appear in the second column and, for example, the trijunction which utilizes edges 1 and 2 has $R \equiv X$, $P \equiv X_1$, and $Q \equiv X_2$. Similarly, (Y, Y_2, Y_3) and (Z, Z_1, Z_3) also generate trijunction subgroups. The generators X_3, Y_1, and Z_2 utilize all edges and have no counterpart on a trijunction. Consistency of braiding and fusion now comes down to graph hexagon equations similar to Eq. (7) in the main text on each subtrijunction, yielding six independent sets of equations. No hexagon equations exist for the generators that involve all three edges. If one tries to commute a fusion vertex through a graph braid involving one of these generators, the fusion vertex will get blocked on the junction point.

Since we just have three independent copies of the graph hexagons for the trijunction, they can be solved as before. However, one can make independent choices of solutions for each set of trijunction hexagon equations. For example, in the case of the Ising fusion rules, one could have, say, $X_\sigma^{\sigma\psi} = +i$ and $Y_\sigma^{\sigma\psi} = Z_\sigma^{\sigma\psi} = -i$. Similarly, for the Fibonacci model, which only allows the usual planar solutions on the trijunction, we can now choose solutions of different chirality on the subjunctions, which yields nonplanar solutions for this model on the tetrajunction. The generators X_3, Y_1, and Z_2, which use all edges, occur in the pseudobraid relation

$$\sigma_2^{(1,2,3)}\,\sigma_1^{(1,3)}\,\sigma_2^{(3,1,2)} = \sigma_1^{(1,2)}\,\sigma_2^{(2,1,3)}\,\sigma_1^{(2,3)}. \tag{A2}$$

This is a graph braiding analog of a Yang-Baxter equation. One may write six such relations for different permutations of (1,2,3), but only one is independent. We can write the pseudobraid relation in terms of the X, Y, and Z symbols by introducing fusion trees at the bottom of the diagrams in Fig. 4. The equality then induces a dodecagonal commutative diagram of F moves and exchanges, similarly to how the equality expressing the compatibility of fusion and braiding induced the graph braiding hexagon equations in Fig. 3 in the main text. This finally gives the following equation:

$$\begin{aligned}
&Y_{1\,fd}^{cba} \sum_{e,g} \left[F_d^{bca}\right]_{fg} Z_g^{ca} \left[\left(F_d^{bac}\right)^{-1}\right]_{ge} X_{3\,ed}^{bac} \left[F_d^{abc}\right]_{ef} \\
&\quad = Y_f^{cb} \sum_{e,g} \left[F_d^{cba}\right]_{fe} X_e^{ba} \left[\left(F_d^{cab}\right)^{-1}\right]_{eg} Z_{2\,gd}^{cab} \left[F_d^{acb}\right]_{gf}.
\end{aligned} \tag{A3}$$

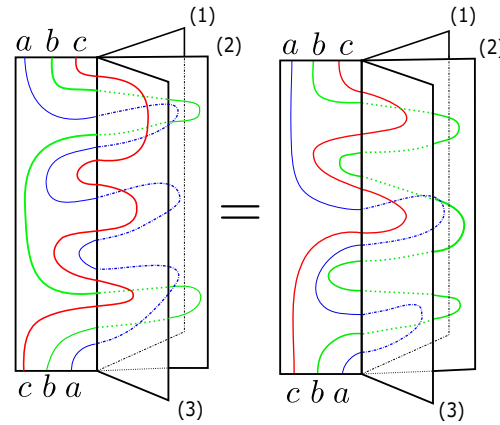

FIG. 4. Graphical representation of the pseudobraid relation on the tetrajunction. The left diagram corresponds to the left-hand side of Eq. (A2), with composition in the equation going vertically in the diagram. The edge assignment for the particles stays fixed throughout the composition on both sides of the equality.

This equation simply allows us to fix the Y_1 symbols in terms of the other symbols. There is never a conflict with the graph hexagons for the trijunctions, as they never involve Y_1. Of course, by choosing a different pseudobraid relation, we could choose to eliminate the X_3 or Z_2 symbols if we prefer. Note that, although we can always eliminate one of the families of symbols that involve all three edges, the other two families are free parameters, as they are not constrained by any further equations. This means that, for example, for Abelian fusion rules governed by a group G, we end up having an extra $2(|G-1)^3$ free parameters in addition to the $3(|G|-1)^2$ parameters coming from the trijunctions. The situation is similar for non-Abelian models: we have free parameters for all of these, although the actual parameter counting is a little more complicated. For example, the Fibonacci model has three free X_3 symbols and three free Z_2 symbols, even though it allows no free parameters at all on the trijunction. Equation (A3) simplifies for Abelian fusion rules. For these, $[F^{abc}_{a\times b\times c}]_{a\times b,b\times c} = \omega(a, b, c)$, where ω is a U(1) valued group 3-cocycle. We find

$$Y_{1\,fd}^{cba}\, c_a(b, c)\, X_{3\,ed}^{bac}\, Z_g^{ca} = Y_f^{cb}\, c_a(c, b)\, X_e^{ba}\, Z_{2\,gd}^{cab}, \tag{A4}$$

where $c_a(b, c)$ is the Slant product

$$c_a(b, c) := (i_a\omega)(b, c) = \frac{\omega(a, b, c)\omega(b, c, a)}{\omega(b, a, c)}. \tag{A5}$$

Often, we can take $c_a(b, c) = c_a(c, b)$; this happens, e.g., for all $\mathbb{Z}_M^\omega$ anyon models. In that case, the Abelian pseudobraid equation does not depend on the F symbols.

Finally we note that we also have new types of gauge-invariant parameters on a tetrajunction: for example, the gauge-invariant quantities $W^{ab}(W')^{ba}$, where $W = \{X, Y, Z\}$ and $W \neq W'$, appear in addition to the parameters W^{aa} and $W^{ab}W^{ba}$ which come from the subtrijunctions.

APPENDIX B: ISING SOLUTION ON A TRIJUNCTION

In this Appendix we will solve the graph hexagon equations for the Ising fusion rules on a trijunction. The planar solutions to the pentagon equations and hexagon equations for

these fusion rules can be found in [2]. There are two nonequivalent sets of F symbols, distinguished by the value of the Frobenius-Schur indicator $\nu = \pm 1$. Most F symbols equal 1. The nontrivial F symbols are $[F_{\psi}^{\sigma\psi\sigma}] = [F_{\sigma}^{\psi\sigma\psi}] = -1$ and

$$\left[F_{\sigma}^{\sigma\sigma\sigma}\right]_{ef} = \frac{\nu}{\sqrt{2}} F(e,f) = \frac{\nu}{\sqrt{2}} \begin{pmatrix} 1 & 1 \\ 1 & -1 \end{pmatrix}, \tag{B1}$$

where $e, f \in \{1, \psi\}$. We first consider the graph hexagon equations in Eq. (7) in the main text with $a = b = c = d = \sigma$. Focusing on the equation for $P_{1\sigma}^{\sigma\sigma\sigma}$ and substituting the F symbols we find that

$$P_{1\sigma}^{\sigma\sigma\sigma} = \frac{\nu}{\sqrt{2}} \left(R_f^{\sigma\sigma}\right)^* F^*(1,f) \sum_e F(1,e) R_{\sigma}^{\sigma e} F(e,f). \tag{B2}$$

We equate the expression for $P_{1\sigma}^{\sigma\sigma\sigma}$ with $f = 1$ to that with $f = \psi$ to get

$$\begin{aligned} P_{1\sigma}^{\sigma\sigma\sigma} &= \frac{\nu}{\sqrt{2}} \left(R_1^{\sigma\sigma}\right)^* \left(R_{\sigma}^{\sigma 1} + R_{\sigma}^{\sigma\psi}\right) \\ &= \frac{\nu}{\sqrt{2}} \left(R_{\psi}^{\sigma\sigma}\right)^* \left(R_{\sigma}^{\sigma 1} - R_{\sigma}^{\sigma\psi}\right). \end{aligned} \tag{B3}$$

Equating the two expressions we get

$$\left(R_1^{\sigma\sigma}\right)^* \left(1 + R_{\sigma}^{\sigma\psi}\right) = \left(R_{\psi}^{\sigma\sigma}\right)^* \left(1 - R_{\sigma}^{\sigma\psi}\right), \tag{B4}$$

which gives us an expression constraining the R symbols directly. Notice that this does not depend on ν, and neither do other equations for the R symbols, so the solutions for R will not detect the dependence on the Frobenius Schur indicator.

Additionally, we can take the Hermitian adjoint of Eq. (B3) to get an expression for $(P_{1\sigma}^{\sigma\sigma\sigma})^{-1}$ and then imposing $P_{1\sigma}^{\sigma\sigma\sigma} \times (P_{1\sigma}^{\sigma\sigma\sigma})^{-1} = 1$ with $f = 1$ we get

$$\begin{aligned} 1 &= \frac{\nu^2}{2} \left(R_1^{\sigma\sigma}\right)^* \left(1 + R_{\sigma}^{\sigma\psi}\right) R_1^{\sigma\sigma} \left[1 + \left(R_{\sigma}^{\sigma\psi}\right)^*\right] \\ &= 1 + \frac{1}{2} \left[R_{\sigma}^{\sigma\psi} + \left(R_{\sigma}^{\sigma\psi}\right)^*\right] \end{aligned} \tag{B5}$$

and hence $(R_{\sigma}^{\sigma\psi})^* = -R_{\sigma}^{\sigma\psi}$, which yields $R_{\sigma}^{\sigma\psi} = \pm i$.

Substituting this back into Eq. (B4), we find that

$$R_1^{\sigma\sigma} = R_{\sigma}^{\sigma\psi} R_{\psi}^{\sigma\sigma} = \pm i R_{\psi}^{\sigma\sigma}. \tag{B6}$$

By equating the expressions for $Q_{1\sigma}^{\sigma\sigma\sigma}$ with $f = 1$ and $f = \psi$ we find

$$\left(R_1^{\sigma\sigma}\right)^* \left(1 + R_{\sigma}^{\psi\sigma}\right) = \left(R_{\psi}^{\sigma\sigma}\right)^* \left(1 - R_{\sigma}^{\psi\sigma}\right). \tag{B7}$$

Comparing Eq. (B7) with (B4) implies $R_{\sigma}^{\sigma\psi} = R_{\sigma}^{\psi\sigma}$, as for the planar solution to the Ising model.

We can tabulate the resulting values for P and Q. The value for $a = b = c = d = \psi$

$$P_{1\psi}^{\psi\psi\psi} = Q_{1\psi}^{\psi\psi\psi} = \left(R_1^{\psi\psi}\right)^*. \tag{B8}$$

Two particles are ψ and one particle is σ:

$$\begin{aligned} P_{\sigma\sigma}^{\sigma\psi\psi} &= Q_{\sigma\sigma}^{\psi\sigma\psi} = \pm i, \\ P_{\sigma\sigma}^{\psi\sigma\psi} &= -Q_{\sigma\sigma}^{\sigma\psi\psi} = \pm i \left(R_1^{\psi\psi}\right)^*, \\ P_{1\sigma}^{\psi\psi\sigma} &= Q_{1\sigma}^{\psi\psi\sigma} = -1. \end{aligned} \tag{B9}$$

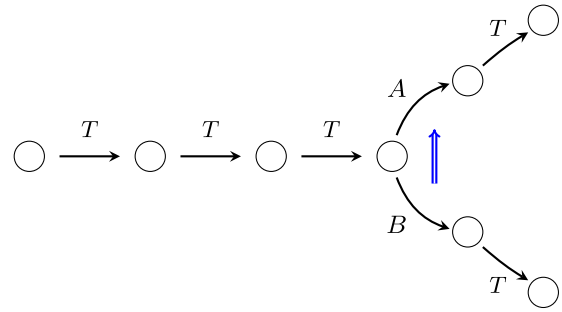

FIG. 5. Here we display a graphical representation for our hopping model. Each circular dot represents a region in the wire which may contain a quasiparticle excitation. We use the blue arrow to denote the ancillary degree of freedom. We also display the lattice sites where our unitary operators act.

Two particles are σ, one particle is ψ, and the total topological charge $d = \psi$:

$$\begin{aligned} P_{\sigma\psi}^{\psi\sigma\sigma} &= Q_{\sigma\psi}^{\psi\sigma\sigma} = \pm i, \\ P_{1\psi}^{\sigma\sigma\psi} &= Q_{1\psi}^{\sigma\sigma\psi} = R_1^{\sigma\sigma}, \\ P_{\sigma\psi}^{\sigma\psi\sigma} &= Q_{\sigma\psi}^{\sigma\psi\sigma} = \pm i. \end{aligned} \tag{B10}$$

Two particles are σ, one particle is ψ, and the total topological charge $d = 1$:

$$\begin{aligned} P_{\sigma 1}^{\psi\sigma\sigma} &= Q_{\sigma 1}^{\sigma\psi\sigma} = \mp i R_1^{\psi\psi}, \\ P_{\sigma 1}^{\sigma\psi\sigma} &= Q_{\sigma 1}^{\psi\sigma\sigma} = \pm i, \\ P_{\psi 1}^{\sigma\sigma\psi} &= Q_{\psi 1}^{\sigma\sigma\psi} = \mp i R_1^{\sigma\sigma}. \end{aligned} \tag{B11}$$

The final configuration has $a = b = c = d = \sigma$:

$$\begin{aligned} P_{1\sigma}^{\sigma\sigma\sigma} &= Q_{1\sigma}^{\sigma\sigma\sigma} = \nu\, e^{\frac{\pm\pi i}{4}} \left(R_1^{\sigma\sigma}\right)^*, \\ P_{\psi\sigma}^{\sigma\sigma\sigma} &= Q_{\psi\sigma}^{\sigma\sigma\sigma} = \nu\, e^{\frac{\mp\pi i}{4}} \left(R_1^{\sigma\sigma}\right)^*. \end{aligned} \tag{B12}$$

The corresponding values for Q^{-1} and P^{-1} are given by Hermitian adjoint. One may check by direct verification that all braid hexagon equations are now satisfied for any choice of $R_1^{\sigma\sigma}$ and $R_1^{\psi\psi}$ in U(1) and for both choices of ν and of the signs. It is interesting to observe that we have $P \neq Q$ whenever $R_1^{\psi\psi} \neq -1$. In other words, $P \neq Q$ unless ψ is a fermion. Nevertheless, even if $R_1^{\psi\psi} = -1$, the solution is usually not planar, as $R_1^{\sigma\sigma}$ is still a free parameter. The possibility of a phase freedom in the exchange of Majorana bound states, given here by $R_1^{\sigma\sigma}$ on a network of quantum wires, has already been discussed in the literature (see, for example, [7,18]).

APPENDIX C: HOPPING MODEL FOR GRAPH BRAIDING ON A TRIJUNCTION

We now introduce a local model of quasiparticles exchanging at a trijunction and we show that it recovers nonplanar solutions of the graph braiding hexagon equations introduced in Eq. (7) the main text.

We will work with quasiparticles labeled by $\mathbb{Z}_2$ charges on a lattice representing a trijunction of wires (see Fig. 5). The presence of a quasiparticle (or an odd number of

quasiparticles) is identified with 1, the nontrivial element of $\mathbb{Z}_2$. The trivial $\mathbb{Z}_2$ charge is denoted 0 and the fusion rules are $1 \times 1 = 0$. At the end of this Appendix we explain how the results are also relevant to Ising-type quasiparticles.

In addition to the presence or absence of a quasiparticle at each lattice position, we also introduce an ancillary pseudospin-$\frac{1}{2}$ degree of freedom (or qubit), displayed as a blue arrow in Fig. 5. A basis for the Hilbert space is then labeled by the possible configurations of quasiparticles on the lattice and one of the two basis states of the ancilla (denoted by arrows pointing up and down below).

We will construct unitary operators hopping the quasiparticles along the wires to implement the exchanges. The idea is that these hopping operators implement adiabatic transport of the quasiparticles as a consequence of some time-varying local perturbation to the Hamiltonian of a lattice model. Graph braiding can be achieved as a composition of a sequence of these hopping operators and we show that this can realize any solution to the graph hexagon equations for $\mathbb{Z}_2$ fusion rules and trivial F symbols.

First, we briefly recall the solutions of the graph hexagon equations for this case. For $\mathbb{Z}_M$ fusion rules with trivial group cocycle (F symbols), these can be written as

$$P_{gd}^{cab} R_f^{cb} = R_d^{ce}, \quad R_g^{ca} Q_{ed}^{bac} = R_d^{fa}. \tag{C1}$$

These equations follow from the graph braiding hexagon equations in Eq. (7) in the main text, with all nonzero F symbols which appear set equal to 1. While it is possible to generalize the entire construction in this section to general M, we now restrict ourselves to the simplest and most important case of $M = 2$. In this case, there is only one nontrivial constraint and it is given by

$$P_{01}^{111} = Q_{01}^{111} = \left(R_0^{11}\right)^*. \tag{C2}$$

We see that we have a graph hexagon solution for any choice of the nontrivial R symbol, $R_0^{11} \in \mathrm{U}(1)$. (Note that $R_1^{10} = R_1^{01} = R_0^{00} = 1$.) In contrast, there are only two solutions to the planar hexagon equations with trivial cocycle, given by $\tilde{R}_0^{11} = 1$ or $\tilde{R}_0^{11} = -1$, as planarity requires simultaneously that $P_{01}^{111} = Q_{01}^{111} = R_0^{11}$.

We now construct the unitary hopping operators. The purpose of the ancilla here is to keep track of how many particles have passed through the junction; as a particle passes the junction, the spin flips 180°. Hence, two particles passing through the junction bring the ancillary back to its initial configuration. In effect, the junction thus keeps track of the $\mathbb{Z}_2$ topological charge passing by.

The actions of the operators A and B, hopping a particle across the junction onto the upper and lower diagonal edges (and back), can now be written

$$\begin{aligned} A\left|\bullet\uparrow \begin{smallmatrix}\circ\\ \circ\end{smallmatrix}\right\rangle &= \theta_u \left|\circ\downarrow \begin{smallmatrix}\bullet\\ \circ\end{smallmatrix}\right\rangle, \qquad A\left|\bullet\downarrow \begin{smallmatrix}\circ\\ \circ\end{smallmatrix}\right\rangle = \theta_d \left|\circ\uparrow \begin{smallmatrix}\bullet\\ \circ\end{smallmatrix}\right\rangle, \\ B\left|\bullet\uparrow \begin{smallmatrix}\circ\\ \circ\end{smallmatrix}\right\rangle &= \psi_u \left|\circ\downarrow \begin{smallmatrix}\circ\\ \bullet\end{smallmatrix}\right\rangle, \qquad B\left|\bullet\downarrow \begin{smallmatrix}\circ\\ \circ\end{smallmatrix}\right\rangle = \psi_d \left|\circ\uparrow \begin{smallmatrix}\circ\\ \bullet\end{smallmatrix}\right\rangle. \end{aligned} \tag{C3}$$

Here $\theta_{u/d}$ and $\psi_{u/d}$ are phase factors picked up by the state as the particle passes through the junction from left to right. The phase accumulated from hopping a particle onto a diagonal edge is dependent on the configuration of the junction point and the subscript label on the phases keeps track of the orientation of the ancilla.

Since A and B are unitary, the phases for passing a particle back from right to left using $A^{-1} = A^\dagger$ and $B^{-1} = B^\dagger$ are also fixed. For example, passing a particle from the upper right branch to the left branch of the junction using A^{-1} will make the state of the system acquire the phase θ_d^{-1}, if the ancilla was in the up state before the exchange.

To make exchanges, we also need to be able to move particles to and from the junctions, on all three wires. For example, directly to the left of the junction, we can now define the action of a unitary operator T, which shuttles particles to and from the junction point by

$$T\left|\bullet\ \circ\uparrow \begin{smallmatrix}\circ\\ \circ\end{smallmatrix}\right\rangle = \left|\circ\ \bullet\uparrow \begin{smallmatrix}\circ\\ \circ\end{smallmatrix}\right\rangle. \tag{C4}$$

Notice that we have not included any phases here. In principle, there can of course be nontrivial phases, but in graph braiding processes, since we always return to the initial configuration, these phases will cancel. We have therefore chosen this simple action to emphasize the effect of exchanging the particles at the junction rather than the dynamical effects of shuttling particles along a quantum wire. Similar T operators will be used to move particles between any pair of neighboring sites on the same wire as needed. Rather than mentioning the relevant sites everywhere below (when it is hopefully clear which sites are meant), we will simply write T for the application of any such operator.

We assume that the action of A, B, and the T operators does not depend on the occupation of any of the other sites, aside from the ones they hop between. We did not need to specify the action A, B, T on states which have the particle already on the right, as we do not need it (A^{-1}, B^{-1}, and T^{-1} are used for moving in the opposite direction). We also did not need to specify how A, B, T act when both sites are filled or empty as we avoid this situation.

To begin an exchange, we first place all particles on the left-hand wire. We denote this state by $|\Omega\rangle$, i.e.,

$$\left|\,\Omega\,\right\rangle = \left|\bullet\ \bullet\ \bullet\uparrow \begin{smallmatrix}\circ\\ \circ\end{smallmatrix}\right\rangle. \tag{C5}$$

Although we display the particles on neighboring sites, in reality they would normally be kept well separated to avoid any nontopological interaction effects during the adiabatic time evolution, implementing this would simply require the use of more of the uninteresting T operators below.

The action of R_0^{11} is now given by the following sequence of hopping operations:

$$R|\Omega\rangle = B^{-1}T^{-1}A^{-1}BTA|\Omega\rangle. \tag{C6}$$

We have decomposed the R symbol into a sequence of hopping moves. This sequence of operators hops a particle onto the upper edge, then brings a particle along the horizontal edge to the junction point and onto the lower edge, and then brings the particle from the upper edge back to the left and away from the junction, followed by the particle from the lower edge. We can see this action is equivalent to the $\sigma_1^{(1,2)}$ graph braid generator depicted in Fig. 1 in the main text. The total phase accumulated by this sequence of hopping moves is

$$R|\Omega\rangle = \theta_u \psi_d \theta_d^{-1} \psi_u^{-1} |\Omega\rangle. \tag{C7}$$

The sequence of hopping operators and phase corresponding to the graph braid generator P_{01}^{111} is similarly given by

$$P_{01}^{111}|\Omega\rangle = A^{-1}T^{-1}T^{-1}B^{-1}T^{-1}T^{-1}A^{-1}BTATTTA|\Omega\rangle = \theta_d\psi_u\theta_u^{-1}\psi_d^{-1}|\Omega\rangle \quad \text{(C8)}$$

and, similarly,

$$Q_{01}^{111}|\Omega\rangle = B^{-1}T^{-1}T^{-1}B^{-1}T^{-1}T^{-1}A^{-1}BTATTTB|\Omega\rangle = \theta_d\psi_u\theta_u^{-1}\psi_d^{-1}|\Omega\rangle. \quad \text{(C9)}$$

If we compare the phases accumulated from the P_{01}^{111} and the Q_{01}^{111} exchanges with the R_0^{11} exchange, we can observe this exactly agrees with Eq. (C2). We can recover the two types of planar exchange statistics with trivial F symbols (bosonic and fermionic) as special cases of this, when $\theta_u\psi_d\theta_d^{-1}\psi_u^{-1} = \pm 1$, i.e., $\theta_u\psi_d = \pm\theta_d\psi_u$. In these cases we recover $P = Q = R$. We can observe that since we come back to the initial state in the Hilbert space, this sequence of unitary operators is tracing out a closed path in the configuration space. As a result of this, the total phase accumulated during the exchanges can not be gauged away. In essence one can interpret this process as a discrete analog of a Berry phase calculation. It is clearly not trivial to come up with physically interesting microscopic models which host localized quasiparticles with $\mathbb{Z}_2$ charges and with protocols for adiabatically transporting these, but nevertheless plausible that braiding in such models can in the end be described using discrete unitary step operators, like the ones we introduced here. Programs for realizing braiding unitaries by adiabatic transport starting from microsopic models have been carried out in detail in the 2D context of the Kitaev honeycomb model [37,38], and also in 1D for Majorana bound states exchanging at a trijunction [7,18].

In the case of the Majorana bound states, there is a $\mathbb{Z}_2$ grading in the Ising-type fusion rules of the model. In effect the σ-type particles have $\mathbb{Z}_2$ charge 1 and both the ψ and vacuum charges have $\mathbb{Z}_2$ charge 0 and this is consistent with the fusion. One may imagine introducing an ancilla qubit at a junction of Majorana wires that is sensitive to this $\mathbb{Z}_2$ charge (i.e., flips when a Majorana mode passes by) and this would allow for a continuous phase degree of freedom to be inserted into the planar braiding solutions that are usually given for the Majorana model. We then notice that this free phase corresponds precisely to the free phase $R_1^{\sigma\sigma}$ which occurs in our graph hexagon solutions, giving an interpretation of this phase as due to a memory effect at the junction. We note that while we modeled our ancilla as a spin at the junction, it does not necessarily have to be an extra degree of freedom, but could be emergent, modeling some characteristic of the underlying system. For example, for Majorana edge modes, the ancilla could keep track of whether the junction point is in the topological or trivial phase of the wire.

[1] A. Y. Kitaev, Fault-tolerant quantum computation by anyons, Ann. Phys. **303**, 2 (2003).

[2] A. Y. Kitaev, Anyons in an exactly solved model and beyond, Ann. Phys. **321**, 2 (2006).

[3] C. Nayak, S. H. Simon, A. Stern, M. Freedman, and S. Das Sarma, Non-Abelian anyons and topological quantum computation, Rev. Mod. Phys. **80**, 1083 (2008).

[4] S. Das Sarma, M. Freedman, and C. Nayak, Topologically Protected Qubits from a Possible Non-Abelian Fractional Quantum Hall State, Phys. Rev. Lett. **94**, 205501 (2005).

[5] H. Bartolomei, M. Kumar, R. Bisognin, A. Marguerite, J.-M. Berroir, E. Bocquillon, B. Placais, A. Cavanna, Q. Dong, U. Gennser, Y. Jin, and G. Féve, Fractional statistics in anyon collisions, Science **368**, 173 (2020).

[6] J. Nakamura, S. Liang, G. C. Gardner, and M. J. Manfra, Direct observation of anyonic braiding statistics, Nat. Phys. **16**, 931 (2020).

[7] J. Alicea, Y. Oreg, G. Refael, F. von Oppen, and M. P. A. Fisher, Non-Abelian statistics and topological quantum information processing in 1d wire networks, Nat. Phys. **7**, 412 (2011).

[8] A. Conlon, D. Pellegrino, J. K. Slingerland, S. Dooley, and G. Kells, Error generation and propagation in Majorana-based topological qubits, Phys. Rev. B **100**, 134307 (2019).

[9] L. Coopmans, D. Luo, G. Kells, B. K. Clark, and J. Carrasquilla, Protocol discovery for the quantum control of Majoranas by differentiable programming and natural evolution strategies, PRX Quantum **2**, 020332 (2021).

[10] Y. Oreg, G. Refael, and F. von Oppen, Helical Liquids and Majorana Bound States in Quantum Wires, Phys. Rev. Lett. **105**, 177002 (2010).

[11] R. M. Lutchyn, J. D. Sau, and S. Das Sarma, Majorana Fermions and a Topological Phase Transition in Semiconductor-Superconductor Heterostructures, Phys. Rev. Lett. **105**, 077001 (2010).

[12] J. D. Sau, S. Tewari, and S. Das Sarma, Universal quantum computation in a semiconductor quantum wire network, Phys. Rev. A **82**, 052322 (2010).

[13] M. S. Scheurer and A. Shnirman, Nonadiabatic processes in Majorana qubit systems, Phys. Rev. B **88**, 064515 (2013).

[14] T. Karzig, G. Refael, and F. von Oppen, Boosting Majorana Zero Modes Phys. Rev. X **3**, 041017 (2013).

[15] M. Cheng, V. Galitski, and S. Das Sarma, Nonadiabatic effects in the braiding of non-Abelian anyons in topological superconductors, Phys. Rev. B **84**, 104529 (2011).

[16] S. S. Hegde, G. Yue, Y. Wang, E. Huemiller, D. J. Van Harlingen, and S. Vishveshwara, A Topological Josephson junction platform for creating, manipulating, and braiding Majorana bound states, Ann. Phys. **423**, 168326 (2020).

[17] B. Bauer, T. Karzig, R. V. Mishmash, A. E. Antipov, and J. Alicea, Dynamics of Majorana-based qubits operated with an array of tunable gates, SciPost Phys. **5**, 004 (2018).

[18] D. J. Clarke, J. D. Sau, and S. Tewari, Majorana fermion exchange in quasi-one-dimensional networks, Phys. Rev. B **84**, 035120 (2011).

[19] U. Khanna, M. Goldstein, and Y. Gefen, Parafermions in a multi-legged geometry: Towards a scalable parafermionic network, Phys. Rev. B **105**, L161101 (2022).

[20] D. Clarke, J. Alicea, and K. Shtengel, Exotic non-Abelian anyons from conventional fractional quantum Hall states, Nat. Commun. **4**, 1348 (2013).

[21] J. M. Leinaas and J. Myrheim, On the theory of identical particles, Il Nuovo Cimento B **37**, 1 (1977).

[22] K. Fredenhagen, K.-H. Rehren, and B. Schroer, Superselection sectors with braid group statistics and exchange algebras. I. General theory, Commun. Math. Phys. **125**, 201 (1989).

[23] J. Fröhlich and F. Gabbiani, Braid statistics in local quantum theory, Rev. Math. Phys. **02**, 251 (1990).

[24] T. Maciążek and A. Sawicki, Non-Abelian quantum statistics on graphs, Commun. Math. Phys. **371**, 921 (2019).

[25] T. Maciążek and B. Hee An, Universal properties of anyon braiding on one-dimensional wire networks, Phys. Rev. B **102**, 201407(R) (2020).

[26] B. H. An and T. Maciążek, Geometric presentations of braid groups for particles on a graph, Commun. Math. Phys. **384**, 1109 (2021).

[27] J. M. Harrison, J. P. Keating, J. M. Robbins, and A. Sawicki, *n*-particle quantum statistics on graphs, Commun. Math. Phys. **330**, 1293 (2014).

[28] G. Moore and N. Seiberg, Classical and quantum conformal field theory, Commun. Math. Phys. **123**, 177 (1989).

[29] T. Maciążek, A. Conlon, G. Vercleyen, and J. K. Slingerland, Extending the planar theory of anyons to quantum wire networks, arXiv:2301.06590.

[30] P. Bonderson, K. Shtengel, and J. K. Slingerland, Interferometry of non-Abelian anyons, Ann. Phys. **323**, 2709 (2008).

[31] M. Freedman, M. Larsen, and Z. Wang, The two-eigenvalue problem and density of Jones representation of braid groups, Commun. Math. Phys. **228**, 177 (2002).

[32] M. Freedman, M. Larsen, and Z. Wang, A Modular functor which is universal for quantum computation, Commun. Math. Phys. **227**, 605 (2002).

[33] D. Tambara and S. Yamagami, Tensor categories with fusion rules of self-duality for finite Abelian groups, J. Algebra **209**, 692 (1998).

[34] J. Siehler, Near-group categories, Algebr. Geom. Topol. **3**, 719 (2003).

[35] S. MacLane, Natural associativity and commutativity, Rice Institute Pamphlet-Rice University Studies **49**, 28 (1963) .

[36] P. Etingof, D. Nikshych, and V. Ostrik, On fusion categories, Ann. Math. **162**, 581 (2005).

[37] V. Lahtinen and J. Pachos, Non-Abelian statistics as a berry phase in exactly solvable models, New J. Phys. **11**, 093027 (2009).

[38] A. Bolukbasi and J. Vala, Rigorous calculations of non-Abelian statistics in the Kitaev honeycomb model, New J. Phys. **14**, 045007 (2012).